PACSIN1 regulates the TLR7/9-mediated type I interferon response in plasmacytoid dendritic cells

Eiji Esashi[*,1], **Musheng Bao**[*,1], **Yi-Hong Wang**[1], **Wei Cao**[1,2], and **Yong-Jun Liu**[1,2]

[1]Department of Immunology and Center for Cancer Immunology Research, The University of Texas M. D. Anderson Cancer Center, Houston, TX, USA

[2]The Graduate School of Biomedical Sciences, The University of Texas, Houston, TX, USA

Abstract

Plasmacytoid dendritic cells (pDCs) are the professional interferon (IFN)-producing cells of the immune system. pDCs specifically express Toll-like receptor (TLR)7 and TLR9 molecules and produce massive amounts of type I IFN by sensing microbial nucleic acids via TLR7 and TLR9. Here we report that protein kinase C and casein kinase substrate in neurons (PACSIN) 1, is specifically expressed in human and mouse pDCs. Knockdown of PACSIN1 by short hairpin RNA (shRNA) in a human pDC cell line significantly inhibited the type I IFN response of the pDCs to TLR9 ligand. PACSIN1-deficient mice exhibited normal levels of conventional DCs and pDCs, demonstrating that development of pDCs was intact although PACSIN1-deficient pDCs showed reduced levels of IFN-α production in response to both cytosine guanine dinucleotide (CpG)-oligonucleotide (ODN) and virus. In contrast, the production of proinflammatory cytokines in response to those ligands was not affected in PACSIN1-deficient pDCs, suggesting that PACSIN1 represents a pDC-specific adaptor molecule that plays a specific role in the type I IFN signaling cascade.

Keywords

Interferon; Plasmacytoid dendritic cells (pDCs); TLR9

Introduction

The innate immune system detects bacterial and viral infection predominantly by sensing their nucleic acids and subsequently producing type I interferon (IFN) [1–3]. During the past decade, major efforts using genomic and genetic approaches have identified two major classes of innate immune receptors for sensing microbial nucleic acids, including Toll-like receptors (TLRs: TLR3, TLR7, TLR8, TLR9) [4, 5] and retinoic acid-inducible gene I-like helicases (RLHs: RIG-I, LGP2, MDA-5) [6, 7]. Recently, a new family of helicases in dendritic cells (DCs) was identified as nucleic acid sensors [8].

Plasmacytoid DCs (pDCs) are the professional IFN-producing cells of the immune system [9–12], specialized in recognizing ribonucleic acid (RNA) and deoxyribonucleic acid (DNA)

from pathogens via the endosomal TLR7 and TLR9, respectively. While TLR7 and TLR9 reside in the endoplasmic reticulum (ER) at steady state, following exposure to nucleic acids, TLR7 and TLR9 relocate from the ER to the endosomes to engage with their RNA or DNA agonists. TLR7 and TLR9 associate with myeloid differentiating factor 88 (MyD88) and conformational changes in the TLRs lead to the activation of MyD88. Activated-MD88 associates with TRAF6 and IRAK4, and the complex further activates NF-κB, IRF5, and IRF7 to propagate the downstream signals [13, 14]. IRF5 and NF-κB cofacilitates the production of proinflammatory cytokines, including IL-6 and TNF [15]. In most cells, IRF7 is induced by IFN via the type I IFN receptor (IFNAR) and the induced-IRF7 further enhances the production of IFN. Remarkably, pDCs constitutively express high levels of IRF7, and the endogenous IRF7 induces rapid type I IFN production without IFNAR-mediated feedback signaling [16].

In a continued effort to study the molecular mechanisms underlying the functional specialization of pDCs in type I IFN-production, we have identified several human pDC-specific molecules by microarray analysis [17], including two pDC-specific receptors (ILT7/ FcεgR1, and BDCA2/FcεgR1) and an intracellular adaptor molecule, protein kinase C and casein kinase substrate in neurons (PACSIN) 1. PACSIN1 belongs to a family of cytoplasmic phosphoproteins that play a role in vesicle formation via their ability to regulate cytoskeletal rearrangement [18]. PACSIN1 is neurospecific, PACSIN2 is ubiquitously expressed, and PACSIN3 is mainly detected in lung and muscle tissues. PACSIN1 that has been implicated as playing a central role in synaptic vesicle recycling, interacts with huntingtin via its C-terminal SRC homology 3 (SH3) domain. All isoforms potentially oligomerize and bind to dynamin, synaptojanin 1 and N-WASP via their SH3 domains [19]. The PACSIN proteins colocalize with dynamin, but not with clathrin, implying a specific role with a distinct subpopulation of dynamin at defined cellular sites. It was also reported that all three PACSIN isoforms bind to endocytic proteins and inhibit endocytosis. Transferrin endocytosis is blocked in a dose-dependent manner in cells overexpressing the PACSIN, but the inhibitory effect can be abolished by mutating specific amino acid residues in the SH3 domains. These characteristics of the PACSIN protein family suggest a general function in recruitment of the interacting proteins to sites of endocytosis. Here, we demonstrate that PACSIN1 represents a pDC-specific adaptor molecule that plays an important role in the TLR7/ TLR9-mediated type I IFN responses by pDCs in vitro and in vivo.

Results and discussion

PACSIN1 is specifically expressed in human pDCs

We have previously identified two surface receptors (ILT7, BDCA2) specifically expressed on human pDCs by microarray analysis [17]. During this study, we also identified an intracellular molecule, called PACSIN1, a member of the PACSIN family, specifically expressed in human pDCs (Supporting Information Fig. 1). We further confirmed this result by real-time PCR; pDCs, mDCs, NK, T, and B cells were isolated and real-time PCR analysis was performed (Fig. 1A). To assess PACSIN1 expression at the protein level, we generated an anti-PACSIN1 monoclonal antibody (mAb) and selective PACSIN1 protein expression in human pDCs was confirmed by western blotting. Isolated pDCs, myeloid DCs (mDCs), NK, T, and B cells were lysed and western blotting was performed with anti-PACSIN1 mAb (Fig. 1B). Further, staining of human tonsil with anti-CD123 Ab and anti-PACSIN1 Ab showed PACSIN1 positive signals were colocalized with CD123 staining (Fig. 1C), indicating that PACSIN1 is specifically expressed in human pDCs at the residential tissue. Taken together, specific expression of PACSIN1 in human pDCs was confirmed at both the mRNA and protein level.

PACSIN1 regulates type I IFN-production in human pDCs

To analyze PACSIN1 function in human pDCs, we performed gene knockdown experiments in a human pDC line Gen2.2, that has been shown to display a phenotype and function identical to that of human primary pDCs [20]. We confirmed that Gen2.2 express PACSIN1 and respond to cytosine guanine dinucleotide (CpG)-oligonucleotide (ODN). We used short hairpin RNA (shRNA) for depletion of PACSIN1 mRNA in Gen2.2 and the reduction of PACSIN1 mRNA by shP1–016 was confirmed (Fig. 2A). PACSIN1 knockdown by shP1–016 led to a strong reduction of IFN-α production in response to CpG-A stimulation (Fig. 2B and C). IFN-α production induced by CpG-B stimulation was moderately blocked by PACSIN1 knockdown, while the induction level by CpG-B was low (Fig. 2C). PACSIN1 knockdown by shP1–016 had no (or marginal) effect on TNF-α production by both CpG-A and CpG-B stimulation (Fig. 2B). These data suggest that PACSIN1 may play a critical role in type I IFN-production induced by TLR9 stimulation, but not in the production of proinflammatory cytokines. Although we examined the activation status of representative signaling molecules, the activation status of those molecules were similar between normal and PACSIN1-deficient cells during CpG stimulation (data not shown).

Analysis of PACSIN1-deficient mice

To determine the precise role of PACSIN1 in vivo, PACSIN1 expression was also analyzed in the mouse. We isolated T cells, B cells, monocytes, mDCs, and pDCs, and quantitative PCR analysis was performed. We found that PACSIN1 was selectively expressed in mouse pDCs. In contrast, PACSIN2 was highly expressed in mDCs and PACSIN3 was ubiquitously expressed (Supporting Information Fig. 2A). Specific expression of PACSIN1 protein was also confirmed in mouse pDCs by western blotting (data not shown). Further, PACSIN1 expression during CpG stimulation was evaluated by quantitative PCR. Expression of PACSIN1 in mouse pDCs was greatly suppressed by CpG-B stimulation but not CpG-A stimulation (Supporting Information Fig. 2B). To evaluate PACSIN1 function in mouse pDCs, we generated PACSIN1 gene-deficient (PACSIN1 knockout (KO)) mice. PACSIN1 gene depletion in KO mice was confirmed by real-time PCR (Supporting Information Fig. 3A). PACSIN1 KO mice developed normally and were fertile (data not shown). PACSIN1 KO and wild-type (WT) mice had a similar number of cells in the thymus, spleen, and bone marrow, and flow cytometric analysis showed PACSIN1 KO mice contained similar number of B cells, T cells, conventional DCs (cDCs), and pDCs in bone marrow and spleen as WT mice (Supporting Information Fig. 3B).

To examine the role of PACSIN1 in mouse pDCs, we isolated pDCs from WT and PACSIN1 KO mice. Isolated pDCs from WT and PACSIN1 KO mice were stimulated with CpG-A and CpG-B. PACSIN1 KO pDCs produced much less IFN-α compared with WT pDCs in response to both CpG-A and CpG-B (Fig. 3A), while no detectable changes between WT pDCs and PACSIN1 KO pDCs were observed in terms of the viability. Further, IL-6 and TNF-α production by both CpG-A and CpG-B was similar between WT and PACSIN1 KO pDCs. These results suggest that PACSIN1 specifically regulates IFN-α but not proinflammatory cytokines production induced by TLR9 ligands in mouse pDCs. To further confirm this, isolated pDCs from WT and PACSIN1 KO mice were stimulated with influenza virus (Flu), vesicular stomatitis virus (VSV), and herpes simplex virus 1 (HSV-1) (Fig. 3B). Indeed, PACSIN1 KO pDCs induced much less IFN-α production in response to each virus compared with that of WT pDCs. Flu and VSV infection is linked to the TLR7-signaling pathway. HSV-1 and CpG activate the TLR9 pathway. Thus, our results indicate that IFN-α production induced by both TLR7- and TLR9-signaling pathways was impaired in PACSIN1-deficient pDCs. Importantly, PACSIN1 deficiency had no effect on the production of other proinflammatory cytokines such as TNF and IL-6. To evaluate the impact of PACSIN1 deficiency in vivo, we performed an HSV-1 infection study in mice

(Fig. 3C). Mice were infected with HSV-1 and cytokine production was measured. As expected, PACSIN1-deficient mice produced much less IFN-α during HSV-1 infection. However, IL-6 production during HSV-1 infection was similar between WT and PACSIN1 KO mice (Fig. 3C). Both WT and PAC-SIN1 KO mice showed no signs of sickness during the infection, suggesting that HSV-1 virus might be cleared even in PACSIN1 KO mice in this experimental condition. Importantly, while the precise role of PACSIN1 during virus rejection is still unclear, PACSIN1 deficiency-exhibited defects in IFN-α induction but not proinflammatory cytokine induction during virus infection in vivo.

Concluding remarks

We have identified PACSIN1 as a pDC-specific adaptor molecule that is critical for the TLR7/TLR9-mediated type I IFN responses to CpG-ODN and viral stimulation in both human and mouse pDCs. Interestingly, PACSIN1 is neither necessary for the induction of proinflammatory cytokines nor for the development of pDC lineage. Our results strongly suggest that PACSIN1 controls the intracellular molecular machinery of IFN-α signaling during CpG or virus infection. The regulation of the signaling complex for IFN-α production is still very mysterious. So far, colocalization of PACSIN1 with TLR7 or TLR9 could not be observed under unstimulated or CpG-stimulated conditions (data not shown), suggesting that PACSIN1 is not directly interacting with the ligands. It has been reported that TLR7/9 localization with early or late endosomes is tightly regulated during CpG or viral stimulation. Thus, it might be possible that PACSIN1 controls the localization of TLR7/TLR9 during the stimulation resulting in IFN-α production. Biochemical characterization of PASCIN1-interacting proteins in pDCs will shed new light on how TLR7/TLR9 signaling by nucleic acids triggers type I IFN production in pDCs.

Materials and methods

Cell isolation from human peripheral blood mononuclear cells

pDCs and mDCs were isolated from the buffy coat of blood from healthy donors as previously described [17]. Briefly, pDCs were sorted by FACS Aria (BD Biosciences, Franklin Lakes, NJ) as Lin^- (CD3, CD14, CD16, CD56, CD19, CD20) $CD4^+$ $CD11c^-$ $CD123^+$, and mDCs were sorted as Lin^- $CD4^+$ $CD11c^+$. Other cell types were sorted accordingly: T cells ($CD3^+$ $CD11c^-$ $CD14^-$ $CD16^-$ $CD19^-$ $CD56^-$), B cells ($CD3^-$ $CD4^-$ $CD8^-$ $CD11c^-$ $CD14^-$ $CD16^-$ $CD19^+$ $CD56^-$), NK cells ($CD3^-$ $CD4^-$ $CD8^-$ $CD14^-$ $CD19^-$ $CD56^+$). This study is approved by the institutional review board for human research at M.D. Anderson Cancer Center.

RNA isolation and quantitative PCR analysis

Reverse transcription and quantitative PCR was performed with specific primer for PACSIN1 (primer sequences are available upon request) as described previously [17]. The expression was normalized with the level of total peripheral blood mononuclear cells (PBMCs). The expression level of each gene in total PBMCs was counted as 1 ($\times$ PBMCs), which means fold change compared with the total PBMCs. A value < 1 indicated the absence of gene expression.

Immunoblot analysis and immunohistochemistry

Whole cell lysates were separated by SDS-PAGE and immunoblots were performed with anti-PACSIN1 Ab. Enhanced chemiluminescence was used for detection.

For immunohistochemical analysis, human tonsil sections were incubated with PACSIN1 antibody followed by Alexa488 conjugated goat antimouse IgG1 (Invitrogen, Carlsbad,

CA). The slides were incubated with biotinylated mouse anti-CD123 mAb and visualized by Alexa549-conjugated streptavidin (Molecular Probes, Carlsbad, CA). Images were acquired by using an inverted microscope, BX41 (Olympus, Tokyo, Japan). Final image processing was performed by using Photoshop (Adobe, San Jose, CA).

Knockdown of PACSIN1 in Gen2.2 cells

Gen2.2 cells were kindly provided by Dr. Joël Plumas (Université Joseph Fourier, Grenoble, France) and cultured as described [20]. Gen2.2 cells were infected with Lentiviral particles targeting PACSIN1 (Open biosystems, Lafayette, CO) or scrambled shRNA (Addgene, Cambridge, MA). Transduced cells were screened and maintained in culture medium containing 1 μg/mL puromycin.

Generation of PACSIN1-deficient mice

Searching the Omni Bank database (http://www.lexgen.com) for ES cell clones with retrovirus insertions in the PACSIN1 gene, we found a clone in which the integration site for the retrovirus was located in the third exon of mouse PACSIN1 gene (clone: OST287788). Animals with targeted disruption of PACSIN1 gene were obtained and back-crossed more than five times with C57BL/6 mice. Mice were genotyped according to manufactures procedures. Heterozygous mice were intercrossed and genotyping was done as described. Further, PACSIN1 gene knockdown was confirmed by real-time PCR (primer sequences for genotyping and real-time PCR are available upon request). Animals were housed in specific pathogen-free barrier facilities. All experiments were performed according to the institutional guidelines at UT MD Anderson Cancer Center.

Antibody staining, isolation of mouse pDCs and in vitro culture of bone marrow

The following antibodies (anti-murine) and reagents were used: FITC-B220, PerCP-Cy5.5-CD11b, APC-CD11c (all from BD Pharmingen), and FITC-PDCA (Miltenyi Biotec, Nordrhein-Westfalen, Germany). Single cell suspensions from bone marrow and spleen were prepared as described previously [21] and analyzed on a FACS-Calibur machine (Becton Dickinson, Franklin Lakes, NJ).

pDCs were isolated from the total bone marrow population by magnetic bead separation followed by fluorescence-activated cell sorting. Lineage-negative bone marrow progenitors (CD3, CD11b, CD19, and Ter119) were recovered by magnetic separation and lin⁻/B220⁺/CD11c⁺ cells (pDCs) were isolated on a FACS Aria machine (BD Biosciences) using FITC-B220, APC-CD11c, and a mixture of PerCP-Cy5.5-labeled CD3, CD11b, and CD19.

For in vitro induction of pDCs, bone marrow cells were cultured in the presence of Flt3L (100 ng/mL, R&D Systems, Minneapolis, MN) for 7 days as described previously [21].

Stimulation of mouse pDCs and in vivo infection study

Freshly isolated mouse pDCs from bone marrow were resuspended in culture medium (4×10^4 cells/100 μL) and stimulated with 1 μM CpG (D19 or 1668), 10^6 pfu of HSV-1, 10^6 pfu of VSV, or 2×10^6 pfu of Flu for 24 h. Supernatants were recovered and cytokine production was measured by ELISA (R&D systems). For in vivo virus infection study, 10^7 pfu of HSV-1 was intravenously injected into WT or PACSIN1-deficient mice. Sera were collected 6 h postinfection and examined for IFN-α production.

Statistical analysis

Data are presented as mean values ± one standard deviation; p-values were calculated using an unpaired two-tailed Student's t-test.

Acknowledgments

Abbreviations

CpG	cytosine guanine dinucleotide
Flu	influenza virus
mDC	myeloid DC
PACSIN	protein kinase C and casein kinase substrate in neurons
pDC	plasmacytoid DC
shRNA	short hairpin RNA
SH3	SRC homology 3
VSV	vesicular stomatitis virus

References

1. Koyama S, Ishii KJ, Coban C, Akira S. Innate immune response to viral infection. Cytokine. 2008; 43:336–341. [PubMed: 18694646]

2. Takeuchi O, Akira S. Innate immunity to virus infection. Immunol. Rev. 2009; 227:75–86. [PubMed: 19120477]

3. Ito T, Wang YH, Liu YJ. Plasmacytoid dendritic cell precursors/type I interferon-producing cells sense viral infection by Toll-like receptor (TLR) 7 and TLR9. Springer Semin. Immunopathol. 2005; 26:221–229. [PubMed: 15592841]

4. Takeda K, Kaisho T, Akira S. Toll-like receptors. Annu. Rev. Immunol. 2003; 21:335–376. [PubMed: 12524386]

5. Kawai T, Akira S. Toll-like receptor and RIG-I-like receptor signaling. Ann. N. Y. Acad. Sci. 2008; 1143:1–20. [PubMed: 19076341]

6. Honda K, Takaoka A, Taniguchi T. Type I interferon [corrected] gene induction by the interferon regulatory factor family of transcription factors. Immunity. 2006; 25:349–360. [PubMed: 16979567]

7. Yoneyama M, Fujita T. RNA recognition and signal transduction by RIG-I-like receptors. Immunol. Rev. 2009; 227:54–65. [PubMed: 19120475]

8. Zhang Z, Kim T, Bao M, Facchinetti V, Jung SY, Ghaffari AA, Qin J, et al. DDX1, DDX21, and DHX36 helicases form a complex with the adaptor molecule TRIF to sense dsRNA in dendritic cells. Immunity. 2011; 34:866–878. [PubMed: 21703541]

9. Siegal FP, Kadowaki N, Shodell M, Fitzgerald-Bocarsly PA, Shah K, Ho S, Antonenko S, et al. The nature of the principal type 1 interferon-producing cells in human blood. Science. 1999; 284:1835–1837. [PubMed: 10364556]

10. Cella M, Jarrossay D, Facchetti F, Alebardi O, Nakajima H, Lanzavecchia A, Colonna M. Plasmacytoid monocytes migrate to inflamed lymph nodes and produce large amounts of type I interferon. Nat. Med. 1999; 5:919–923. [PubMed: 10426316]

11. Fitzgerald-Bocarsly P, Dai J, Singh S. Plasmacytoid dendritic cells and type I IFN: 50 years of convergent history. Cytokine Growth Factor Rev. 2008; 19:3–19. [PubMed: 18248767]

12. Swiecki M, Colonna M. Accumulation of plasmacytoid DC: roles in disease pathogenesis and targets for immunotherapy. Eur. J. Immunol. 2010; 40:2094–2098. [PubMed: 20853492]

13. Uematsu S, Sato S, Yamamoto M, Hirotani T, Kato H, Takeshita F, Matsuda M, et al. Interleukin-1 receptor-associated kinase-1 plays an essential role for Toll-like receptor (TLR)7- and TLR9-mediated interferon-{alpha} induction. J. Exp. Med. 2005; 201:915–923. [PubMed: 15767370]

14. Kawai T, Akira S. TLR signaling. Cell Death Differ. 2006; 13:816–825. [PubMed: 16410796]

15. Takaoka A, Yanai H, Kondo S, Duncan G, Negishi H, Mizutani T, Kano S, et al. Integral role of IRF-5 in the gene induction programme activated by Toll-like receptors. Nature. 2005; 434:243–249. [PubMed: 15665823]

16. Kerkmann M, Rothenfusser S, Hornung V, Towarowski A, Wagner M, Sarris A, Giese T, et al. Activation with CpG-A and CpG-B oligonucleotides reveals two distinct regulatory pathways of type I IFN synthesis in human plasmacytoid dendritic cells. J. Immunol. 2003; 170:4465–4474. [PubMed: 12707322]

17. Cao W, Rosen DB, Ito T, Bover L, Bao M, Watanabe G, Yao Z, et al. Plasmacytoid dendritic cell-speci.c receptor ILT7-Fc epsilonRI gamma inhibits Toll-like receptor-induced interferon production. J. Exp. Med. 2006; 203:1399–1405. [PubMed: 16735691]

18. Qualmann B, Kelly RB. Syndapin isoforms participate in receptor-mediated endocytosis and actin organization. J. Cell Biol. 2000; 148:1047–1062. [PubMed: 10704453]

19. Sumoy L, Pluvinet R, Andreu N, Estivill X, Escarceller M. PACSIN 3 is a novel SH3 domain cytoplasmic adapter protein of the pacsin-syndapin-FAP52 gene family. Gene. 2001; 262:199–205. [PubMed: 11179684]

20. Chaperot L, Perrot I, Jacob MC, Blanchard D, Salaun V, Deneys V, Lebecque S, et al. Leukemic plasmacytoid dendritic cells share phenotypic and functional features with their normal counterparts. Eur. J. Immunol. 2004; 34:418–426. [PubMed: 14768046]

21. Esashi E, Wang YH, Perng O, Qin XF, Liu YJ, Watowich SS. The signal transducer STAT5 inhibits plasmacytoid dendritic cell development by suppressing transcription factor IRF8. Immunity. 2008; 28:509–520. [PubMed: 18342552]
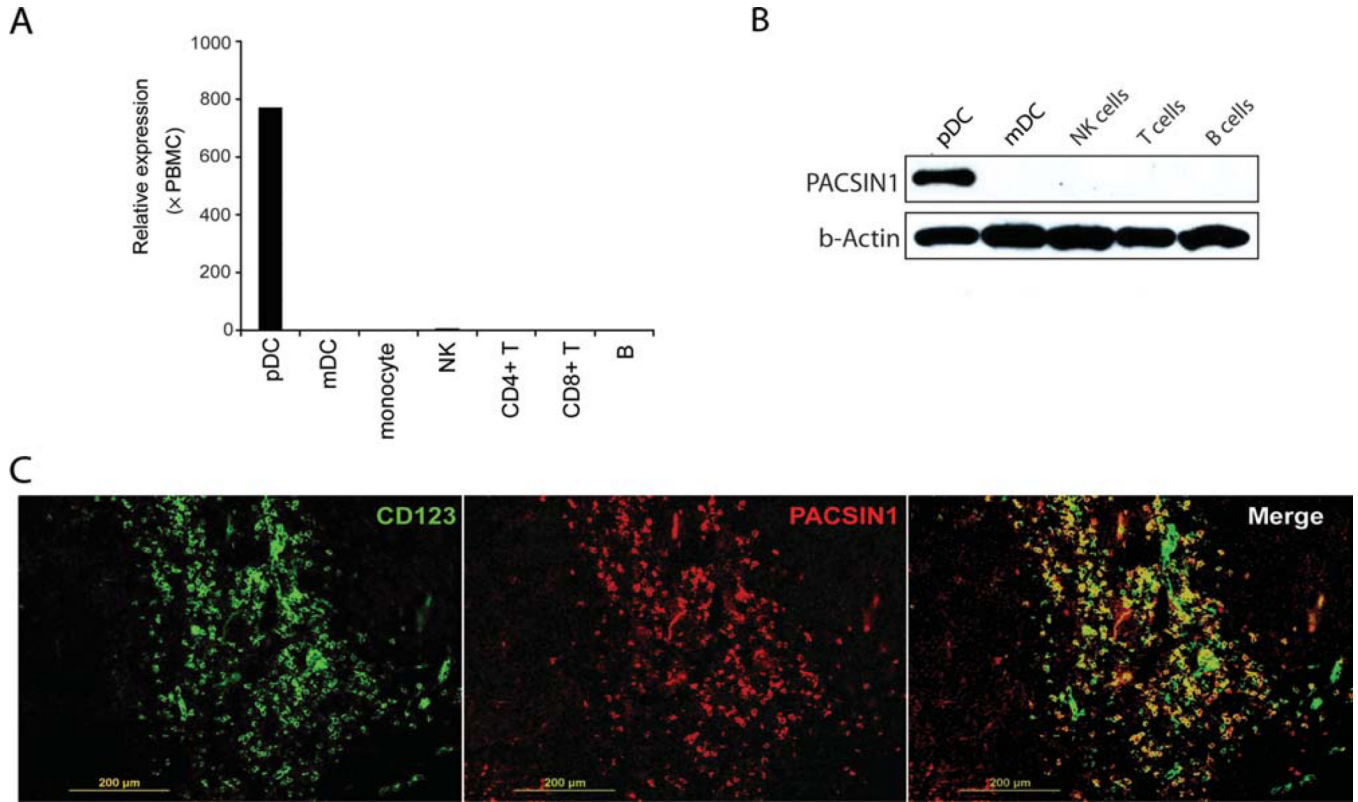
Figure 1. Analysis of PACSIN1 expression in human pDCs and other immune cells
(A) Human pDCs, mDCs, monocytes, NK, T, and B cells were isolated from PBMCs, and total RNA was purified from each. The cDNA was subjected to quantitative PCR analysis. The relative gene expression of PACSIN1 on different cell types was determined by quantitative RT-PCR analysis. The expression was normalized with that of total PBMCs. The expression level of each gene in total PBMCs was counted as 1; × PBMCs means fold change compared with PBMCs. (B) The expression levels of PACSIN1 in human pDCs, mDCs, NK, T, and B cells were analyzed by western blot with an anti-PACSIN1 antibody. β-actin was used as a loading control. (C) Human paraffin-embedded tonsil sections were stained with biotin-labeled anti-CD123 antibody and anti-PACSIN1 antibody, followed by Alexa Fluor® 549 Streptavidin and Alexa Fluor® 488 conjugated goat antimouse IgG1. Images were acquired by using an inverted microscope, BX41. Scale bar, 200 μm. Results are representative of two independent experiments.
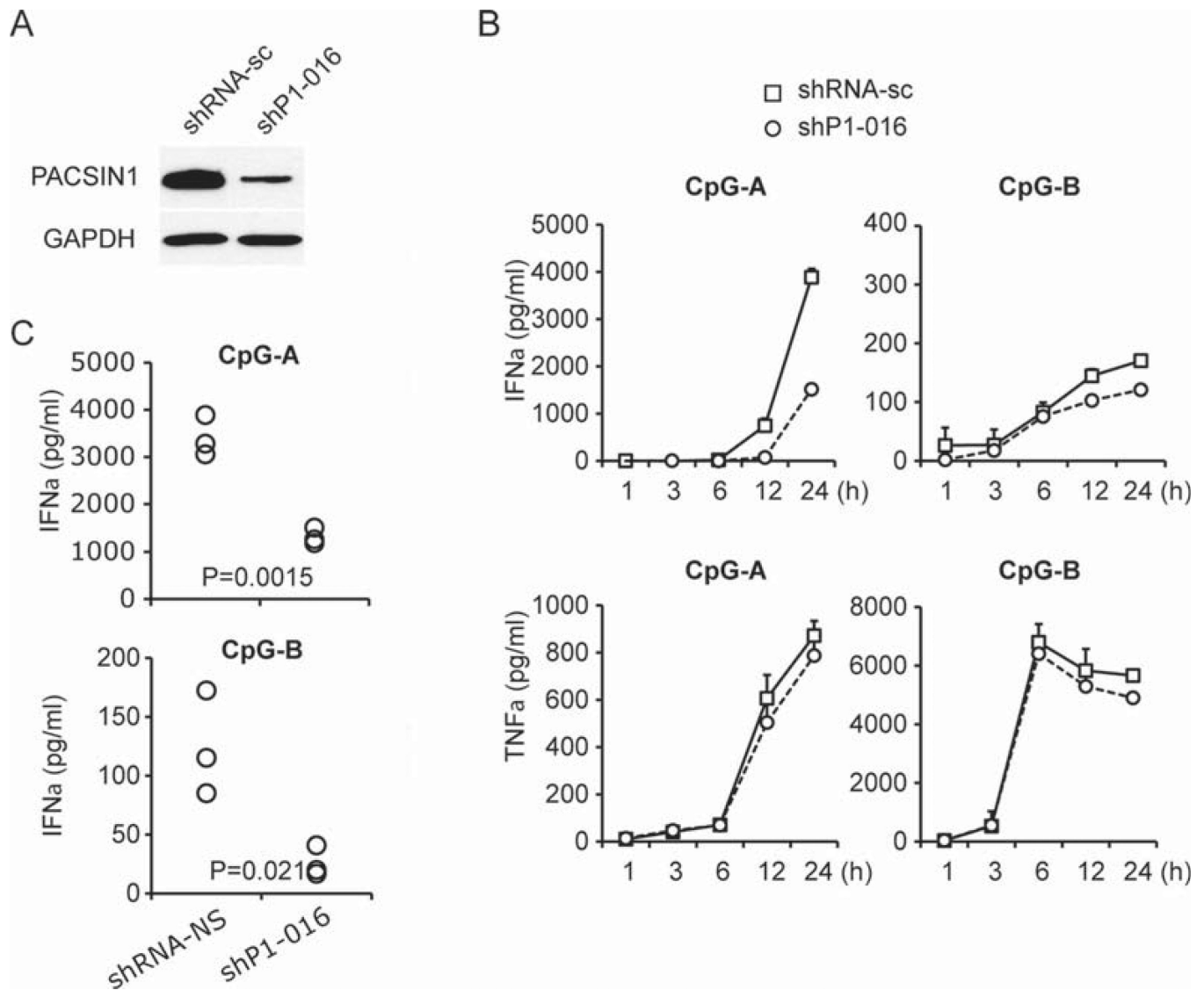
Figure 2. Effects of PACSIN1 knockdown on the response to TLR9 ligands
(A) Gen2.2 cells were transduced with scrambled shRNA (shRNA-sc) or shRNA targeting
PACSIN1 (shP1–016). The knockdown effect of PACSIN1 was confirmed by western blot
and GAPDH was used as a loading control. Representative result from one of three
independent experiments is shown. (B) shRNA transduced Gen2.2 cells were stimulated
with 1 μM CpG-A (left panel) or 0.5 μM CpG-B (right panel) for 1 h, 3 h, 6 h, 12 h, 24 h.
Levels of IFN-α, TNF-α, and IL-6 in the culture supernatants were measured by ELISA.
Results are from one experiment representative of three. Error bars show mean+SD of
triplicates. Statistical analysis was performed using an unpaired two-tailed Student's *t*-test.
(C) Levels of IFN-α production at 24 h stimulation with CpG-A (upper) or CpG-B (lower)
in PACSIN1-knockdown or control Gen2.2 cells were measured by ELISA. Each symbol
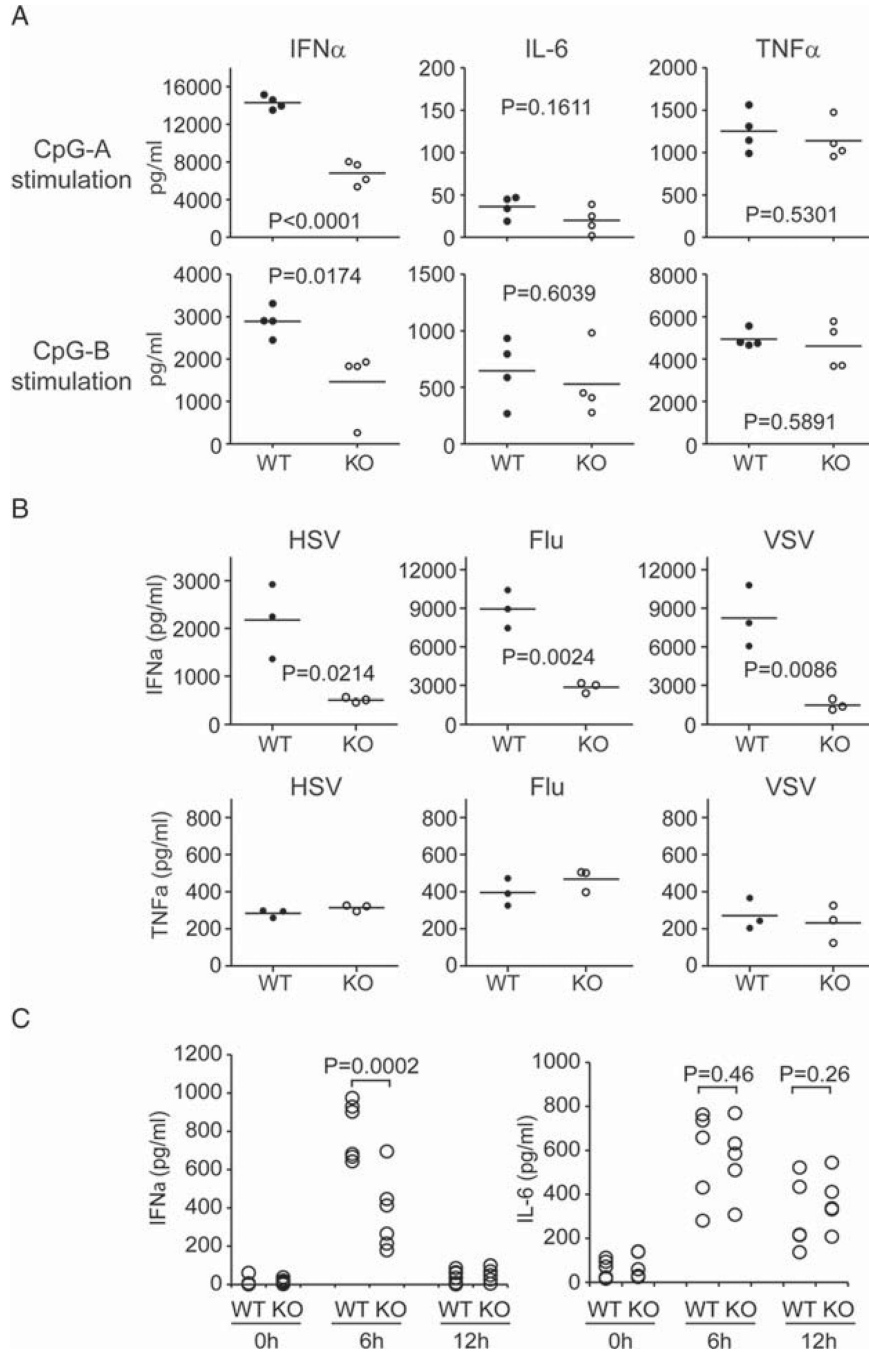represents one independent experiment.

Figure 3. PCASIN1-deficient pDCs display severely impaired IFN-α production
(A) pDCs isolated from WT and PACSIN1-deficient mice were stimulated with 1 μM of CpG-A and CpG-B for 24 h. Cytokine production (IFN-α, TNF-α, and IL-6) was measured by ELISA. The data represent cytokine production by pDCs from individual mice (circle, *n* = 4/genotype). (B) Isolated pDCs were stimulated with Flu, VSV, and HSV-1 for 24 h. IFN-α and TNF-α production was measured by ELISA. The data represent pDCs from individual mice (circle, *n* = 3/genotype). A representative result of two independent experiments is shown. (C) WT and PACSIN1-deficient mice were injected intravenously via tail vein with 1×10^7 pfu HSV-1 virus. Sera were collected 6 h and 12 h after infection. Induction of IFN-α (left panel) and IL-6 (right panel) in the sera were measured by ELISA.

Sera before virus infection were used as baseline control. Each circle represents one mouse (n = 6 per group). Statistical analysis was performed using an unpaired two-tailed Student's t-test.